Solution Structure of FK506 Bound to the R42K, H87V Double Mutant of FKBP-12

Christopher A. Lepre, David A. Pearlman, Jya-Wei Cheng, Maureen T. DeCenzo, David J. Livingston, and Jonathan M. Moore*

Vertex Pharmaceuticals Incorporated, 40 Allston Street, Cambridge, Massachusetts 02139-4211

Received June 13, 1994; Revised Manuscript Received August 25, 1994®

ABSTRACT: The binding of the FK506/FKBP-12 complex to calcineurin (CN), its putative target for immunosuppression, involves recognition of solvent-exposed regions of the ligand as well as FKBP-12 residues near the active site. The R42K, H87V double mutation of FKBP-12 decreases the CN affinity of the complex by 550-fold [Aldape, R. A., Futer, O., DeCenzo, M. T., Jarrett, B. P., Murcko, M. A., & Livingston, D. J. (1992) *J. Biol. Chem. 267,* 16029−16032]. This work reports the solution structure of ^{13}C-labeled FK506 bound to R42K, H87V FKBP-12. Assignments and NOE measurements at three mixing times were made from inverse-detected $^{1}H-^{13}C$ NMR experiments. Structures were calculated by several different methods, including distance geometry, restrained molecular dynamics, and molecular dynamics with time-averaged restraints. The NMR structures of the ligand are very well defined by the NOE restraints and differ slightly from the X-ray structure in regions that are involved in crystal packing. Comparison with the NMR structure of FK506 bound to wild-type FKBP-12 reveals that the R42K, H87V mutation causes the ligand backbone near C16 to move by 2.5 to 4.5 Å, reorients 15-MeO by 90°, and shifts 13-MeO by approximately 1.5 Å. FK506 appears to undergo a concerted, mutationally induced shift in the binding pocket, with the greatest changes occurring in the effector region of the drug. The altered effector conformation of mutant-bound FK506 may perturb interactions between the drug and CN, thus accounting for the effect of the double mutation upon the CN inhibitory activity of the complex.

FK506 (tacrolimus) is a fungal macrolide (Figure 1) that impedes early events in the Ca^{+2}-dependent activation of T cells (reviewed by Schreiber, 1991; Rosen & Schreiber, 1992; and Sigal & Dumont, 1992). This potent, immunosuppressant drug binds to a family of homologous proteins that range in size from 12 to 52 kDa (Siekierka et al., 1989; Harding et al., 1989; Jin et al., 1991; Galat et al., 1992; Peattie et al., 1992). The most widely studied of the FK506 binding proteins (FKBPs) is FKBP-12[1] (11.8 kDa), for which the structures of the native protein (Moore et al., 1991; Michnick et al., 1991) and the FK506 complex (Van Duyne et al., 1991, 1993) have been reported. The FK506/FKBP-12 complex interferes with cytoplasmic signal transduction by binding and inhibiting calcineurin, a calcium- and calmodulin-dependent protein phosphatase (Liu et al., 1991, 1992; Fruman et al., 1992; O'Keefe et al., 1992; Clipstone & Crabtree, 1992). Since calcineurin is not inhibited by either FK506 or FKBP-12 alone (Liu et al., 1991), considerable effort has been directed toward elucidating the structural features of the FK506/FKBP-12 complex responsible for calcineurin inhibition.

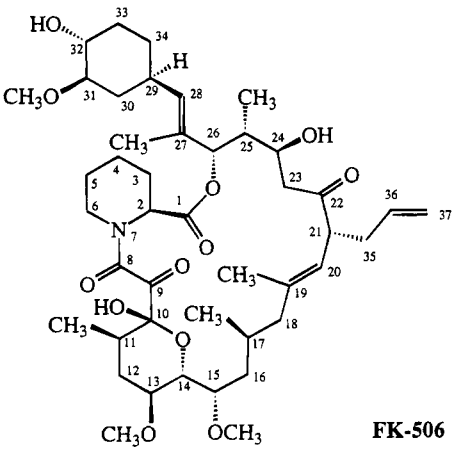

FIGURE 1: Primary structure of FK506.

An early model for the structural basis of inhibition by the FK506/FKBP complex proposed that the drug possesses two main structural elements: a protein binding domain and an effector domain that is recognized by a downstream target (Schreiber, 1991). This model was supported by the work of Bierer et al., (1990), in which a synthetic ligand lacking an effector domain failed to block T-cell activation, although it successfully competed with FK506 in binding and inhibiting the rotamase activity of FKBP-12. Later, an X-ray crystallographic study of the FK506/FKBP complex revealed that the putative effector domain (C17 to C22 and allyl region) of FK506 projects outward from the surface of the protein into the solvent (Van Duyne et al., 1991, 1993). Lastly, chemical modifications of 15-MeO and the allyl group were shown to dramatically reduce the ability of the complex to inhibit calcineurin phosphatase activity (Liu et al., 1992).

* Author to whom correspondence should be addressed.

® Abstract published in *Advance ACS Abstracts,* October 15, 1994.

[1] Abbreviations: 2D, two dimensional; COSY, 2D homonuclear correlated spectroscopy; CVFF, constant valence force field; DG, distance geometry; FKBP-12, human recombinant FK506 binding protein (11.8 kDa); FKBP-13, human recombinant FK506 binding protein (13.2 kDa); HMQC, 2D heteronuclear multiple-quantum coherence; HSQC, 2D heteronuclear single-quantum coherence; IL-2, interleukin-2; MD, molecular dynamics; NOE, nuclear Overhauser effect; NOESY, 2D nuclear Overhauser effect spectroscopy; NMR, nuclear magnetic resonance; RMSD, root mean square deviation; TARMD, time-averaged restrained molecular dynamics; TOCSY, 2D total correlation spectroscopy.

0006-2960/94/0433-13571$04.50/0

Recent structural and mutational studies of the FK506/FKBP-12 complex have subsequently revised the original "effector domain" hypothesis (Schreiber, 1991). The original model did not consider contributions by the protein in providing surface sites that could be recognized by calcineurin. However, Aldape et al. (1992) showed that several surface residues near the bound ligand are important for calcineurin inhibition. Based upon these and subsequent mutational studies (Aldape et al., 1992; Yang et al., 1993; Rosen et al., 1993; Rotonda et al., 1993), a modified model has emerged in which residues of the 40−44 (40s) and 84−91 (80s) loops of FKBP-12, as well as the original "effector domain" of FK506, are believed to be involved in forming a composite surface that is recognized by calcineurin.

Although the calcineurin affinity of the wild-type FKBP-12 complex is highly sensitive to modification of the protein or ligand, inactive complexes of other FKBPs have been modified to create potent new calcineurin inhibitors. For example, the complex of 18-OH ascomycin (a close FK506 analog whose FKBP-12 complex does not inhibit calcineurin) with yeast FKBP-12 is a potent inhibitor (Rotanda et al., 1993). Also, the complex of FKBP-13 with FK506 only weakly inhibits calcineurin, but substitution by the 40s loop from FKBP-12 (Rosen et al., 1993) or introduction of three point mutations (O. Futer and D. Livingston, unpublished results) confers strong activity.

The FK506 complexes of several R42 mutants possess considerably weaker calcineurin inhibitory activity than wild-type, but their FK506 binding affinities remain unaffected. For example, the R42K and R42I mutants have K_i's for calcineurin that are 107-fold and 176-fold lower than wild-type, respectively (Aldape et al., 1992). The H87V substitution decreases calcineurin inhibition by only 4-fold, while H87F, H87L, and H87A mutants have wild-type activity (Aldape et al., 1992; Yang et al., 1993). However, when the R42K and H87V mutations are both present, the affinity of the complex for calcineurin decreases by 550-fold (Aldape et al., 1992).

This paper reports the solution structure of FK506 bound to the R42K, H87V double mutant of human recombinant FKBP-12, as determined by NMR spectroscopy. By comparing the conformations of FK506 bound to double mutant and wild-type-bound protein, a structural mechanism can be proposed that accounts for the effect of the double mutation upon calcineurin inhibition by the FK506/FKBP-12 complex.

MATERIALS AND METHODS

Data Collection and Restraint Generation. All data were collected at 303 K on a Bruker AMX-500 spectrometer as described previously (Lepre et al., 1992), using a sample of 3.2 mM ^{13}C-FK506/human recombinant FKBP-12 complex in 50 mM potassium phosphate/D_2O buffer at pD 7.4. Data were processed with FELIX software (Biosym Technologies, San Diego, CA), and peak assignment and integration were carried out using the EASY program (Eccles et al., 1989). The ^{1}H and ^{13}C resonances of protein-bound ^{13}C-FK506 were assigned using ^{13}C COSY, HSQC, HMQC-TOCSY (τ_m = 32 ms), and HSQC-NOESY (τ_m = 40, 60, and 100 ms) spectra as described previously (Lepre et al., 1992).

Six of the eight pairs of methylene protons were stereospecifically assigned (all but 23-CH_2 and 35-CH_2) by comparing the NOE intensities observed in 40 and 60 ms HSQC-NOESY spectra with interproton distances measured from the best of a preliminary set of 200 distance geometry structures calculated from 40 and 60 ms NOE restraints.

The structure of bound FK506 was calculated from a composite set of 93 NOE distance restraints that were derived from NOE intensities measured in HSQC-NOESY spectra with mixing times of 40 ms (58 restraints), 60 ms (20 restraints), and 100 ms (15 restraints). Use of 60 and 100 ms NOE restraints was limited to long-range distances that did not involve the ring systems in order to minimize spin diffusion effects. The NOE intensities were scaled to account for the number of attached protons, as well as the level of ^{13}C enrichment at the site of origin (Lepre et al., 1992). The restraints at each mixing time were calibrated internally within each data set in order to avoid errors associated with scaling raw data. A conservative calibration was used to convert NOE intensities into upper bounds by taking the weakest NOEs between neighboring ring methylene protons to be 3.03 Å (*trans* orientation). Instead of using pseudoatoms for methylene pairs, equivalent restraints were applied to both protons, and 1.7 Å was added to the upper bounds. Lower bounds of 1.8 Å were used in all cases. The six dihedral angles within the pipecolinyl ring were restrained to within ±60° of values consistent with the chair conformer. The amide bond was restrained to the *trans* orientation only for the DG calculations.

Distance Geometry Calculations. Bound FK506 structures were generated from the NOE distance and dihedral angle restraints using the DGII distance geometry algorithm with triangle smoothing (Havel, 1991) within InsightII (Biosym Technologies, San Diego, CA). Preliminary sets of structures were calculated (using pseudoatoms for all methylenes) from the original 40 ms NOE restraints and recalculated each time new restraints (from 60 ms, 100 ms data) were added, in order to check for restraint violations and consistency of the structures. A final set of 200 DGII structures was generated using restraints from all three mixing times, stereospecific assignments, and dihedral angle restraints.

Molecular Dynamics Refinement within Discover. Restrained molecular dynamics refinement of 33 DGII structures of receptor-bound FK506 having the lowest error functions (no distance restraint violations >0.02 Å) was carried out within Discover (Biosym Technologies). These calculations were carried out on FK506 alone (no model of FKBP), using the CVFF all-atom force field and a distance-dependent dielectric to simulate solvent effects. The same restraint set was employed as for the DGII calculations, except that the *trans* amide dihedral restraint was not used. Each structure was first minimized using 1000 steps of unrestrained steepest descents and then heated to 1500 K over 1 ps while linearly increasing the force constants for the NOE distance and dihedral angle restraints from zero to their maximum values. After equilibrating for 8 ps at 1500 K (time step of 2 fs), the system was cooled exponentially to 300 K over 7 ps, followed by a final 2000 steps of restrained conjugate gradients minimization. The NOE restraint penalties followed a biharmonic function for interproton distances that violated the upper or lower bounds. Dihedral angles lying outside the limits were penalized by a function of the form $K[1 + \cos(\phi - \phi_0)]$, where ϕ_0 is the limit of the allowed range and K = 30 kcal mol^{-1} rad^{-2}.

Restrained Molecular Dynamics within AMBER. Restrained molecular dynamics calculations of the FK506

structure in the explicitly modeled FKBP-12 active site were carried out using the AMBER/SANDER 4.0 program (Pearlman et al., 1991). The calculations employed an all atom force field with a distance-dependent dielectric and an 8 Å nonbonded cutoff. The same restraint set was used as for the Discover refinement, except that very weak ($k = 1.0$ kcal/mol Å^2) harmonic positional restraints were applied to the C8 and C9 carbonyls in order to prevent the ligand from drifting out of the active site during the calculations. The tendency for the ligand to drift out the active site results from the fact that explicit solvent was not included in the calculations (D. A. Pearlman, unpublished results). The starting structure was either the X-ray structure of FK506 bound to the R42K, H87V double mutant (S. Itoh, M. DeCenzo, R. Aldape, D. Livingston, D. Pearlman, and M. Navia, unpublished results) or a hybrid constructed from the wild-type X-ray conformation of FK506 (Van Duyne et al., 1991) docked onto double mutant FKBP-12 by superimposing the pipecolinyl cores. Prior to performing restrained MD, the starting structures were energy-minimized in the presence of the NMR restraints ($k = 20$ kcal/mol Å^2), with the protein structure fixed. MD calculations were run using either strong (60 kcal/mol Å^2) or weak (7.5 kcal/mol Å^2) force constants, and the protein was kept fixed at all times. Covalent bond lengths were constrained with SHAKE (Ryckaert et al., 1977), and a time step of 2 fs was used. Sets of 10 minimized starting structures were subjected to the following protocol (using full nonbonded interactions): the system was heated linearly from 300 to 900 K over 2 ps, while linearly increasing the force constant for the restraints from 10% to their maximum values over 4 ps. With the restraint force constant fixed at maximum value, the system was then allowed to equilibrate for 8 ps at 900 K, and then cooled exponentially to 300 K over 6 ps.

Time-Averaged Restraint Simulations. Molecular dynamics simulations of FK506 bound to double mutant FKBP-12 using time-averaged restraints were carried out by using AMBER/SANDER 4.0 (Pearlman et al., 1991). The averaging formula employed (Torda et al., 1989; Pearlman, 1994) was of the form

$$\langle r_{\text{model}}(t')\rangle = \left[\frac{\int_0^{t'} e^{(t-t')/\tau}\, r_{\text{model}}(t)^{-3}\, dt}{\int_0^{t'} e^{(t-t')/\tau}\, dt}\right]^{-1/3}$$

where the time constant for the damping factor (τ) was 10 ps. Pseudoforces (Torda et al., 1990; Pearlman & Kollman, 1991) were applied using a force constant of 7.5 kcal/mol Å^2 and the same restraint set as was used in the standard MD refinement. Starting structures for the simulations were the same as described above for the standard AMBER calculations. In addition, the structure of FK506 bound to wild-type FKBP-12 was calculated using the X-ray structure of the wild-type complex (van Duyne et al., 1991) as the starting conformation and the NOE restraint set used in a previous study (Lepre et al., 1992). All simulations consisted of 500 ps of dynamics carried out with a time step of 2 fs, at a constant temperature of 300 K. At every 1000th step (2 ps) the current structure was saved to an archive file. The average structure was calculated by best-fitting and averaging all of the structures in the archive except for those saved within the first 20 ps of the simulation (to avoid equilibration effects) (Pearlman, 1994).

RESULTS

Structures Obtained by MD Refinement in Discover. The conformation of FK506 bound to double mutant FKBP-12 is well defined in structures calculated using several computational strategies. This is primarily due to the large number of NOE-derived distance restraints that are applied to this small molecule (126 atoms). In addition, unrestrained MD simulations of free FK506 indicate that the macrocycle backbone and the cyclohexyl group are sterically hindered (Pranata & Jorgensen, 1991; Pearlman, 1994), thus inherently limiting the range of conformers accessible to the molecule.

The 33 distance geometry structures having the lowest residual errors are shown in Figure 2a. These structures have a mean pairwise RMSD from the average structure of 0.93 Å for all heavy atoms. Upon restrained MD refinement, 27 of the 33 structures adopt a *trans* amide conformation, suggesting that the bound drug prefers the *trans* amide conformation, as it does when bound to wild-type FKBP-12 (Lepre et al., 1992). The 12 MD-refined structures with the lowest total energies and the lowest violations of the NOE restraints (none > 0.3 Å) are shown in Figure 2b. These structures have a mean RMSD from the average structure of 0.47 Å for all heavy atoms, and all possess a *trans* amide conformation. Separate refinements were run with strong (60 kcal mol^{-1} Å^{-2}) and with weak (10 kcal mol^{-1} Å^{-2}) force constants (k) in order to test for unusual strain in the structures. The final energies of the refined structures were the same regardless of whether strong or weak penalties were employed, indicating that the structures were not being forced to adopt covalently strained conformations in order to satisfy the restraints.

The density of restraints is lowest in the regions of the pipecolinyl, the allyl group, and the macrocycle backbone from C22 to C24. For the pipecolinyl, this lack of restraints is due to the absence of isotopic labeling in the ring, which prevented the assignment of the pipecolinyl resonances in the HSQC-NOESY spectrum. The chemical shifts of the pipecolinyl resonances of the double mutant and wild-type complexes are almost identical, however, indicating that the binding cores are similarly oriented, and in the current structure determination neither the protein binding pocket nor pipecolinyl restraints were needed in order for the pipecolinyl to adopt a well-defined orientation. Upon MD refinement, the pipecolinyl ring (in the energetically preferred chair conformer) moved into a position that was similar to that seen in the X-ray structures of the wild-type and double mutant FKBP-12 complexes, indicating that the influence of the force field alone is sufficient to define the pipecolinyl orientation relative to the rest of the macrocycle.

The low number and intensity of NOEs involving the allyl group, as well as the narrow line widths observed for its NMR resonances, indicate that it is highly mobile. Heteronuclear and homonuclear relaxation experiments reveal that the allyl group in the wild-type FK506/FKBP-12 complex is solvent-exposed and disordered on the picosecond time scale (Lepre et al., 1993). Since this group is not in contact with the protein in the wild-type complex, it is expected to be equally mobile in the double mutant.

The macrocycle backbone is not well ordered at C22 and C23 because there are no protons, and hence no restraints, at C22, and also because the methylene protons of C23 could not be stereospecifically assigned. The increased disorder

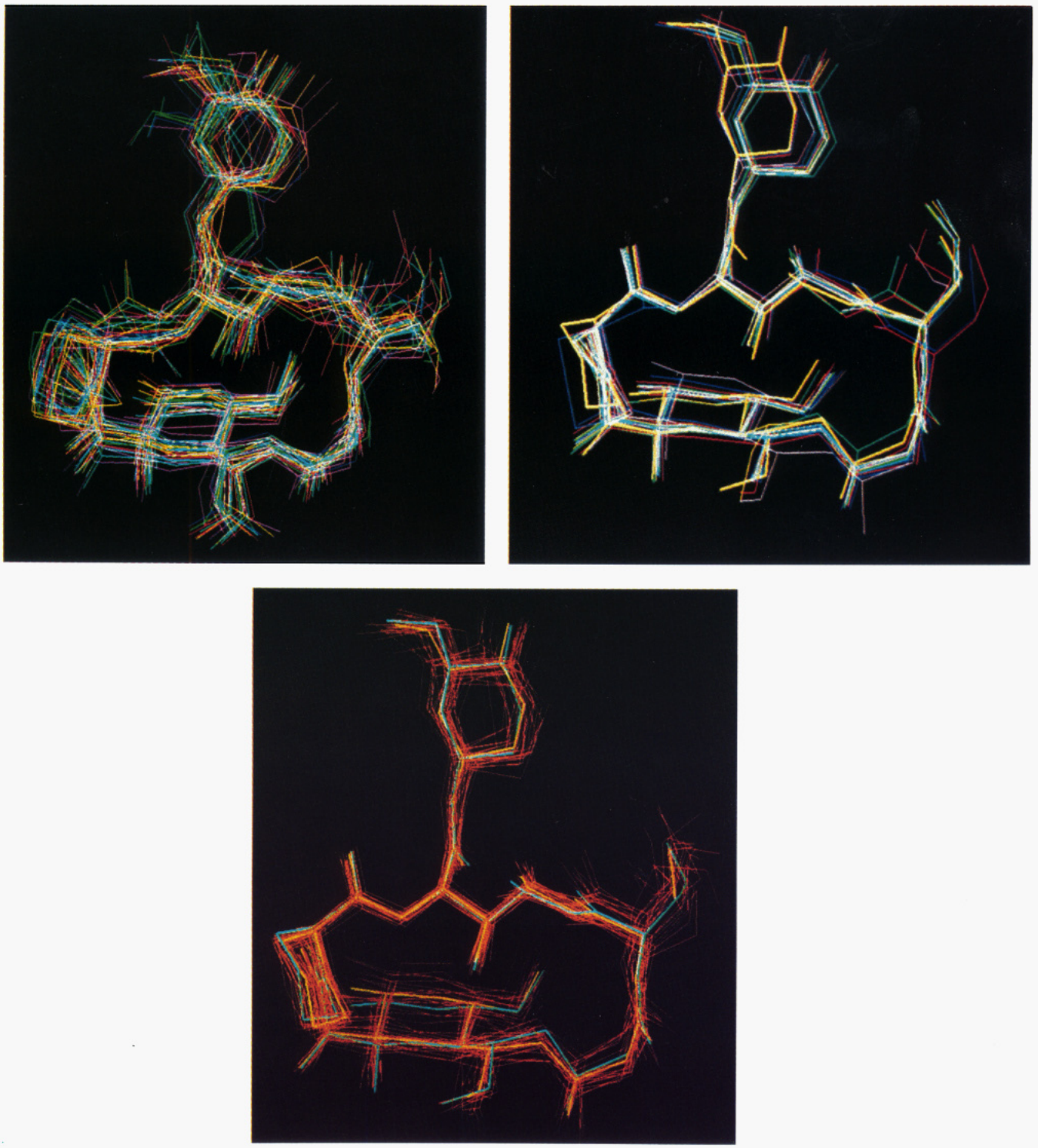

FIGURE 2: (a, top left) All (heavy) atom superposition of the 33 distance geometry structures of FK506 that have the fewest NOE restraint violations. Only heavy atoms are shown. (b, top right) Superposition of the 12 MD-refined (Discover, $k = 10$ kcal/mol Å^2) NMR structures (various colors), with the lowest energy structure obtained from restrained MD in AMBER (yellow). (c, bottom) Family of 25 structures sampled during time-averaged restrained MD simulation (amber), the average structure (yellow), and the lowest energy structure obtained from conventional restrained MD in AMBER (blue).

seen in this region of the family of MD-refined NMR structures may thus be due to the lower density of restraints, as well as possibly reflecting real conformational disorder in the bound ligand. The adjoining regions of the macrocycle, however, are well ordered.

The orientation of the cyclohexyl group is defined relative to the macrocycle backbone by NOE restraints connecting the ring protons with H28 and 27-Me on the trisubstituted olefin, which are in turn connected to H13, 13-MeO, H24, and H26. The overall fold of the macrocycle backbone is defined by a set of long-range NOE restraints from 27-Me to H13 and 13-MeO, from 25-Me to H13, H15, and 19-Me, and from H25 to H16. It is in the region of the macrocycle backbone between the pyranose ring and the allyl group that the NMR structures differ most from the X-ray structures of both the double mutant and wild-type complexes. Fortunately, this is also the best-restrained region of the molecule. The protons of C13 through C19 are heavily

restrained by a dense network of NOE restraints (over half of the total restraints), and the structures are consequently well defined in this region.

Restrained Molecular Dynamics within AMBER. As seen in Figure 2b, restrained MD refinement of the DG structures in the absence of protein produces a set of final structures that occupy a relatively narrow conformational envelope. During calculations of the structure of FK506 bound to wild-type FKBP-12 (Lepre et al., 1992), it was observed that the standard MD refinement protocol resulted in highly converged families of structures. This was partly attributed to the final energy minimization step, which tends to reduce families of structures with differing local structures to common, lowest energy conformers. In addition, it was noted that restrained MD refinement of a bound ligand in the absence of its receptor may cause poorly restrained regions to adopt conformations that reflect the force field of the free ligand.

In order to assess whether the presence of the receptor influences the resulting structures, a second set of structure calculations was performed with the ligand in the binding pocket using AMBER. These calculations employed a full force field (all atoms, all nonbonded interactions) and had no final minimization step. A number of different starting structures and restraint penalties were used, as described in Materials and Methods. The best structures (having the lowest AMBER energies and no violations of the distance restraints) were obtained when the starting conformation was the X-ray structure of the double mutant complex and the system was allowed to equilibrate under the influence of relatively weak (7.5 kcal/Å^2) NOE force constants. When strong (60 kcal/Å^2) force constants were applied, the structures exhibited slightly larger deviations from ideal covalent geometry. As was seen for standard MD refinement, the lowest energy structures consistently adopted the chair conformer of the pipecolinyl and *trans* amide geometry, even when no dihedral angle restraints were used. When the starting structure was the wild-type conformation of FK506 docked onto double mutant FKBP-12, the ligand structures became trapped in higher energy minima (regardless of whether strong or weak NOE penalties were used), possibly because reorientation of the backbone near C15 would have required the transient violation of a large number of restraints.

Figure 2b shows the superposition of the lowest energy structure obtained by restrained MD calculation of the bound ligand structure within AMBER with the 12 best structures obtained by Discover MD refinement in the absence of protein. The structures obtained from the two different methods are very similar, with an average pairwise RMSD between the Discover-refined structures and the AMBER structure of only 0.54 Å for heavy atoms. Restrained MD calculations using AMBER in the absence of protein yielded similar results (not shown). These results demonstrate that the restraint set is sufficient to define the ligand conformation independent of the force field or the presence of the receptor in the calculations.

By keeping the protein fixed during the refinement at the position observed in the X-ray structure of the double mutant complex, the assumption was made that the conformation of the binding pocket in solution was essentially the same as in the solid state. This assumption is not unreasonable, since the side-chain positions of residues buried in the binding pocket are the same in the NMR structure of ascomycin (a close FK506 analog) bound to FKBP-12 as in the X-ray structure of FK506 bound to FKBP-12 (Meadows et al., 1993). In addition, significant differences between the solution and crystal structures of the protein binding pocket would be expected to give rise to differences between the NMR structures calculated on and off of the protein, and would likely produce covalent strain and/or restraint violations in the bound ligand structures. None of these effects were observed, indicating that any differences between the solution and crystal positions of the binding pocket residues are insufficient to affect the internal conformation of the bound ligand.

Time-Averaged Restraint Simulations. Previous studies have shown that time-averaged restrained MD (TARMD) samples the conformational space accessible to bound FK506 more efficiently than conventional restrained MD methods (Pearlman, 1994). In order to avoid problems with convergence to local minima that were encountered when conventional MD was previously used to refine bound FK506 structures (Lepre et al., 1992), and to allow for the possibility of time-averaging of the measured NOE intensities by ligand motions, MD simulations were carried out using time-averaged restraints within AMBER.

A representative family of 25 conformers sampled during the course of a TARMD simulation of bound FK506 is shown in Figure 2c. During the course of this simulation, which used the X-ray structure of the double mutant complex as the starting conformation, the AMBER energies of the structures fluctuated by 5.5 kcal/mol^{-1} (RMS), and the average energy was comparable to that observed in the structures obtained by conventional AMBER refinement. The RMS violation of the NOE distance restraints during the run was only 0.024 Å, and the RMS violation of the dihedral angle restraints was 0.59°. The average structure obtained by TARMD was essentially the same as the best structure obtained by standard MD refinement in AMBER, with an RMS difference between them of only 0.37 Å for all heavy atoms (Figure 2c).

A duplicate time-averaged restrained MD simulation was run with a different set of random starting velocities in order to check that the ensemble converged to the same average structure. The RMSD between the average structures from the two runs was only 0.085 Å for all heavy atoms, indicating that a 500 ps simulation is sufficient to achieve thorough sampling.

Another simulation was run by starting from the wild-type conformation of FK506 docked onto double mutant FKBP-12. This control run converged to the same average structure as was obtained by starting from the X-ray structure of the double mutant (RMSD between them of only 0.11 Å for all heavy atoms). Thus, TARMD refinement was better able to avoid becoming trapped in local minima than standard MD refinement, presumably because momentary violations of the restraints are tolerated as long as the time-average of the distances is satisfied. It should be noted, though, that time-averaged refinement is generally less efficient than conventional MD at converging upon an average conformation in cases where it starts from a poor initial guess (Pearlman & Kollman, 1991).

The individual RMSDs of the heavy atom positions from their mean positions during the TARMD run are depicted in Figure 3. Above-average RMSDs are observed in three

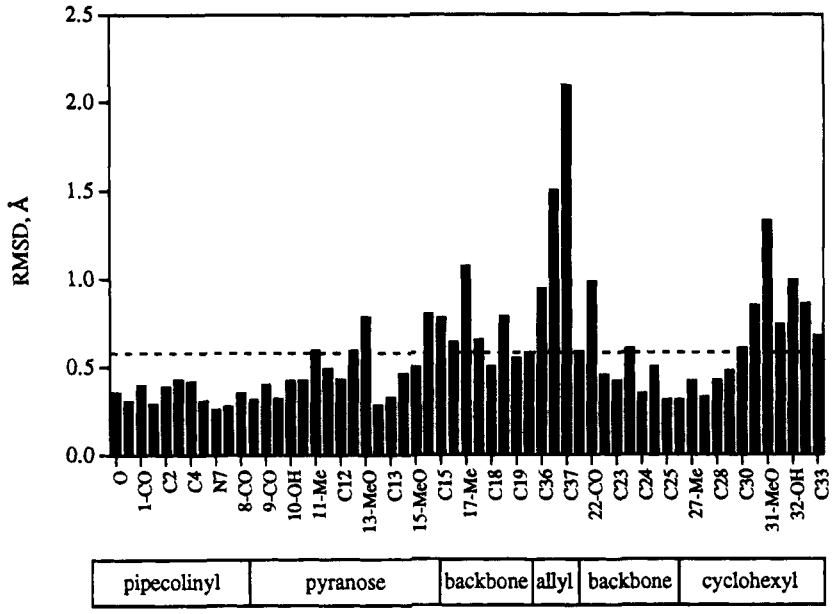

FIGURE 3: Fluctuations in the positions of the heavy atoms of FK506 bound to double mutant FKBP-12 during the course of a 500 ps time-averaged restrained MD trajectory. Values are plotted as RMS deviations from the mean heavy atom positions. The dotted line represents the average RMSD value over the entire ligand.

regions of the molecule: the macrocycle backbone from C14 to C16, the allyl group, and the cyclohexyl group. The set of FK506 structures sampled during the run has an average pairwise RMSD from the mean structure of 0.64 Å for all heavy atoms, which is larger than the corresponding RMSD measured from the family of structures obtained by conventional MD refinement (0.47 Å). This result is consistent with the expectation that time-averaged MD simulations better reflect the full range of conformers accessible to the ligand, and further supports the notion that traditional static depictions of the ligand give an incomplete description of the three-dimensional structure (Pearlman, 1994). For this reason, the TARMD results are used for most of the following discussion of the wild-type and double mutant structures.

Comparison with the Solution Structure of the Wild-Type Complex. The set of FK506 structures sampled during TARMD refinement of the wild-type complex has an average pairwise RMSD from the mean structure of 0.69 Å and RMS violations of the NOE and dihedral angle restraints of 0.15 Å and 0.40°, respectively. The energies of the structures fluctuated by 4.7 kcal/mol^{-1} (RMS) during the run. As reported previously, the wild-type X-ray and NMR structures are generally similar, except for differences in the allyl region (C21 shifted by about 1.2 Å) that are thought to arise from crystal packing effects (Lepre et al., 1992).

Figure 4a illustrates the superposition of the solution conformers of FK506 bound to wild-type and double mutant FKBP-12, created by superimposing the backbone atoms of the protein. It is important to note that the binding cores of the ligands superimpose precisely, regardless of whether they are oriented relative to the wild-type or the double mutant protein backbone. This is not unexpected, since the structures of both the ligand binding cores and the protein backbones are very similar in the X-ray structures of these two complexes (S. Itoh, M. DeCenzo, R. Aldape, D. Livingston, D. Pearlman, and D. Navia, unpublished results). This result confirms, however, that the ligand does not shift in the binding pocket during the course of the TARMD simulation, despite the use of relatively weak positional restraints on the dicarbonyl. Also, it confirms that the superposition based on the protein backbone is reasonable for comparing the NMR and X-ray structures.

Overall, the wild-type and double mutant-bound ligand structures present the same global fold, but exhibit local structural variations in regions outside of the binding core. The two families of structures (Figure 4a) deviate from one another to varying degrees in the vicinity of the allyl group, the cyclohexyl ring, the pyranose ring, and the macrocycle backbone between the pyranose and allyl groups.

In two of the regions where the families of structures differ, ^{13}C relaxation studies have shown that elevated mobility exists in the wild-type complex (Lepre et al., 1993). The allyl group of FK506 in both complexes is highly mobile, and most likely undergoes free rotation about the C21−C35 bond. The cyclohexyl group of FK506 undergoes a wagging motion in both TARMD simulations (Figure 4b), consistent with relaxation studies of the wild-type complex that show that this group has above average mobility, but does not undergo a full 180° ring flip (Lepre et al., 1993). Because the envelopes of conformers produced by these motions overlap, it appears that the ligands can freely sample conformers in the vicinity of both average cyclohexyl conformations in solution at room temperature. So, the slight differences seen between the average cyclohexyl orientations in the two families of NMR structures, and those seen between the wild-type and double mutant crystal structures, do not appear to be physically significant.

The most important differences between the wild-type and the double mutant structures occur in the conformation of the macrocycle backbone between the pyranose and allyl groups (Table I and Figure 4c). As seen in Figure 4c, the family of wild-type conformers lies well outside of the envelope of conformers that is accessible to the ligand when bound to double mutant FKBP-12. These different families of conformers are uniquely defined by their NOE restraint sets: the wild-type NOE restraints always produce the wild-type structure, and the double mutant restraints always give

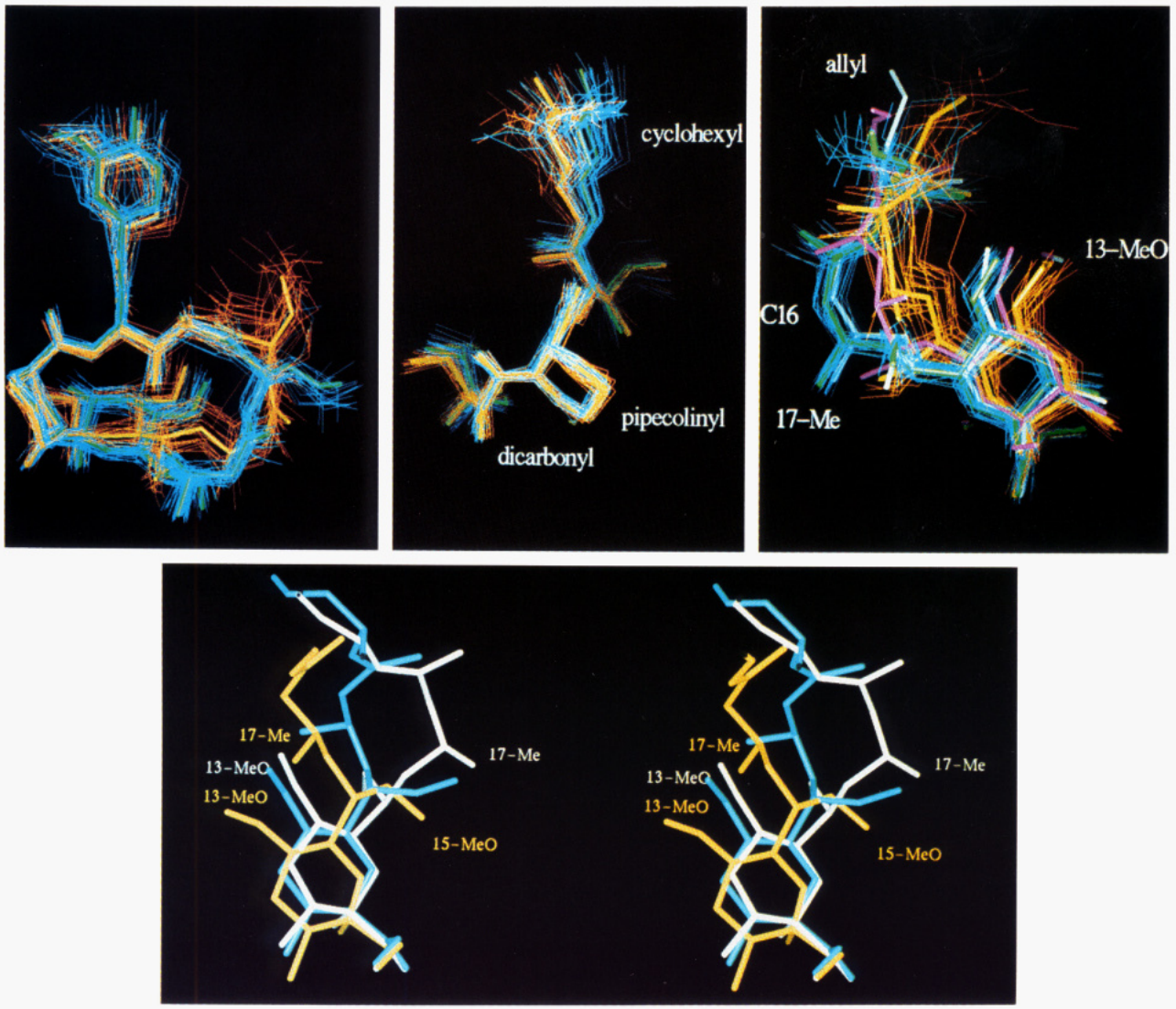

FIGURE 4: (a, top left) Comparison of the family of 25 structures sampled during TARMD simulation of FK506 bound to double mutant FKBP-12 (amber, with average structure in yellow) with the family sampled by FK506 bound to wild-type FKBP-12 (blue, with average structure in green). Superposition is based upon the protein backbone heavy atoms. (b, top center) View of the pipecolinyl−dicarbonyl binding core and the cyclohexyl group. (c, top right) View of the macrocyle backbone linking the pyranose and allyl groups, including the X-ray structure of FK506 bound to wild-type (white) and double mutant (purple) FKBP-12. (d, bottom) Comparison of the X-ray structure of FK506 bound to wild-type (white) and double mutant (blue) FKBP-12 and the lowest energy structure obtained from restrained MD in AMBER of FK506 bound to double mutant FKBP-12 (yellow).

Table 1: Comparison of Selected Backbone Torsion Angles (deg) in FK506/FKBP-12 Complexes

	carbons in torsion			
structure	13−14−15−16	14−15−16−17	15−16−17−18	17−18−19−20
wild-type X-ray[a]	42	168	92	−100
wild-type MD[b]	68	168	70	−88
wild-type TARMD[c]	63 (8)[h]	181 (7)	68 (6)	−80 (9)
double mutant X-ray[d]	−117	122	13	−166
double mutant MD[e]	−41 (4)	−89 (3)	177 (10)	−99 (2)
double mutant MD[f]	−46	−87	175	−103
double mutant TARMD[g]	−43 (11)	−103 (28)	−180 (14)	−97 (14)

[a] From van Duyne et al. (1991). [b] From Lepre et al. (1992). [c] This work; average structure from MD simulation with time-averaged restraints. [d] S. Itoh, M. DeCenzo, R. Aldape, D. Livingston, D. Pearlman, and M. Navia, unpublished results. [e] This work; average of the 12 best structures obtained by MD refinement using Discover, with no protein present. [f] This work; best structure from standard MD refinement using AMBER, with the protein present. [g] This work; average structure from MD simulation with time-averaged restraints. [h] Standard deviation in parentheses.

the double mutant structure, regardless of which X-ray conformation of the bound ligand is used as the starting structure for TARMD.

The deviations in the macrocycle backbone of double mutant-bound FK506 (Figure 4d) center about the C15−C16 and C16−C17 torsions, so that the orientation of 15-MeO in the lowest energy AMBER structure (as defined by the value of the C13−C14−C15−O torsion), differs by 92° from wild type. As a result, in the double mutant 15-MeO and 13-MeO lie on opposite sides of the plane defined by the macrocycle ring. The differences in the torsion angles about C16 change the direction of the backbone in the region

from C16 to C18. Based upon a superposition of the binding core, C16 is displaced by approximately 2.5 Å, C17 by 4 Å, and C18 by 4.5 Å from their positions in the wild-type structure. The orientation of 17-Me is reversed, so that it lies on the same side of the macrocycle ring plane as 13-MeO. Accompanying these changes is a small, but significant, rotation of the pyranose ring. Because the family of conformers sampled by the pyranose is relatively narrow in both complexes, it can be seen (Figure 4c) that this shift is most pronounced for the side of the ring opposite the dicarbonyl linkage, and it causes 13-MeO to move toward the Val 87 pocket by about 1.5 Å.

The observed structural changes in the ligand are reflected by changes in the proton chemical shifts. The protons of C11, 11-Me, and C12 on the pyranose ring and C16 on the backbone show the largest differences in chemical shift between the wild-type and double mutant bound forms ($\Delta\delta$ > 0.25 ppm for all).

Comparison with the Crystal Structure of the Double Mutant Complex. The solution and crystal structures of FK506/FKBP-12 complexes are typically very similar in the region of the ligand binding core (pipecolinyl and dicarbonyl). The FK506 binding cores from the wild-type and double mutant crystal structures (Van Duyne et al., 1991, 1992; Itoh, S., DeCenzo, M., Aldape, R., Livingston, D., Pearlman, D., and Navia, M., unpublished results) may be superimposed upon the average TARMD structure to give heavy atom RMSDs of 0.13 Å and 0.16 Å, respectively. Although the solution and crystal structures of the double mutant complexes are grossly similar, they differ in the conformations of the allyl group, the cyclohexyl ring, and the macrocycle backbone between the pyranose ring and the allyl group. These regions of the ligand all make intermolecular contacts in the crystal (S. Itoh, M. DeCenzo, R. Aldape, D. Livingston, D. Pearlman, and M. Navia, unpublished results).

In solution, the allyl group of FK506 in the double mutant complex appears to be highly mobile, and the cyclohexyl group is expected to have elevated mobility as well, as found in the wild-type complex (Lepre et al., 1992, 1993). However, in the X-ray structures of both complexes, these groups are well ordered (Van Duyne et al., 1991, 1993; S. Itoh, M. DeCenzo, R. Aldape, D. Livingston, D. Pearlman, and M. Navia, unpublished results). The different orientations and mobilities of the allyl group in the crystal and solution structures can be attributed to the fact that, in the crystal, the allyl group is involved in extensive intermolecular packing interactions. Likewise, the exposed edge of the cyclohexyl ring is also involved in intermolecular crystal contacts. As seen in Figure 4b, this ring undergoes a wagging motion in the TARMD simulation, consistent with the mobility studies of the wild-type complex. However, there is no evidence of cyclohexyl mobility in either of the X-ray structures, again presumably due to crystal packing effects. Further support for this conclusion comes from the X-ray structure of FK506 bound to triple mutant FKBP-13 (J. Griffith, K. Wilson, and M. Navia, unpublished results), in which the cyclohexyl ring makes no crystal contacts and exhibits low electron density and elevated temperature factors.

The NMR and X-ray structures differ most in the values of the backbone torsion angles about C16. The fact that the X-ray conformation of double mutant-bound FK506 does not satisfy the NMR restraints supports this conclusion, as several distances in the C16 region are violated by more than 0.5 Å. In addition, the C15−C16 and C16−C17 torsions both differ by over 130°, causing a change in the direction of the backbone that shifts C16 by ca. 1.7 Å (Table I and Figure 4d). Again, the differences between the NMR and X-ray structures can be attributed to the effects of intermolecular crystal packing. In the solid state, the region from the pyranose ring to the allyl group makes numerous contacts with the same region of an opposing complex in the unit cell, with 15-Me contacting 13-MeO (S. Itoh, M. DeCenzo, R. Aldape, D. Livingston, D. Pearlman, and M. Navia, unpublished results). Despite the differences between the solution and crystal structures, the NMR structure of double mutant-bound FK506 resembles the X-ray structure of the double mutant complex more closely than it does the X-ray or NMR structures of the wild-type complex, particularly with regard to the altered orientations of 15-MeO and 17-Me.

It is interesting to note that the family of structures for double mutant-bound FK506 is less well defined in the vicinity of C16 than the wild-type family. This is surprising, since there are more NOE restraints in this region for the double mutant structures (due to higher quality NOE data). It is possible that this disorder reflects an increase in conformational mobility that is mutationally induced. It is important to keep in mind, though, that although mobility will give rise to disorder in a family of TARMD structures, observation of such disorder alone does not prove that mobility exists. Independent confirmation of mobility in this region may be provided by ^{13}C relaxation measurement of the ligand dynamics.

DISCUSSION

In solution, FK506 binds to R42K, H87V FKBP-12 in a single conformation. The ligand structures obtained from several different computational approaches are very similar, and are all typified by well-defined structures, few or no violations of the input restraints, and good agreement with ideal covalent geometry. The average structure obtained from MD refinement using time-averaged distance restraints is the same as the average of the family of structures obtained by conventional MD refinement. This result implies that the conventional and time-averaged refinements populate qualitatively similar families of conformers, since the calculated average position would be shifted if the ligand sampled a conformation that was dramatically outside the TARMD family. The mean RMSD is larger for the TARMD structures, however, indicating that TARMD produces a family that more efficiently samples the ensemble of energetically reasonable states accessible to the ligand.

Although the NMR and X-ray structures of FK506 bound to double mutant FKBP-12 are virtually identical in the pipecolinyl−dicarbonyl core region, they exhibit differences in the solvent-exposed regions of the ligand. These differences are greatest in the macrocycle backbone near C16. This region is of particular interest because it is near the side chain of Arg 42 in the wild-type X-ray structure and thus is likely to be structurally affected by the side-chain substitution. In addition, this region of the ligand backbone includes 15-MeO, which is thought to be an important site for calcineurin recognition (Liu et al., 1992).

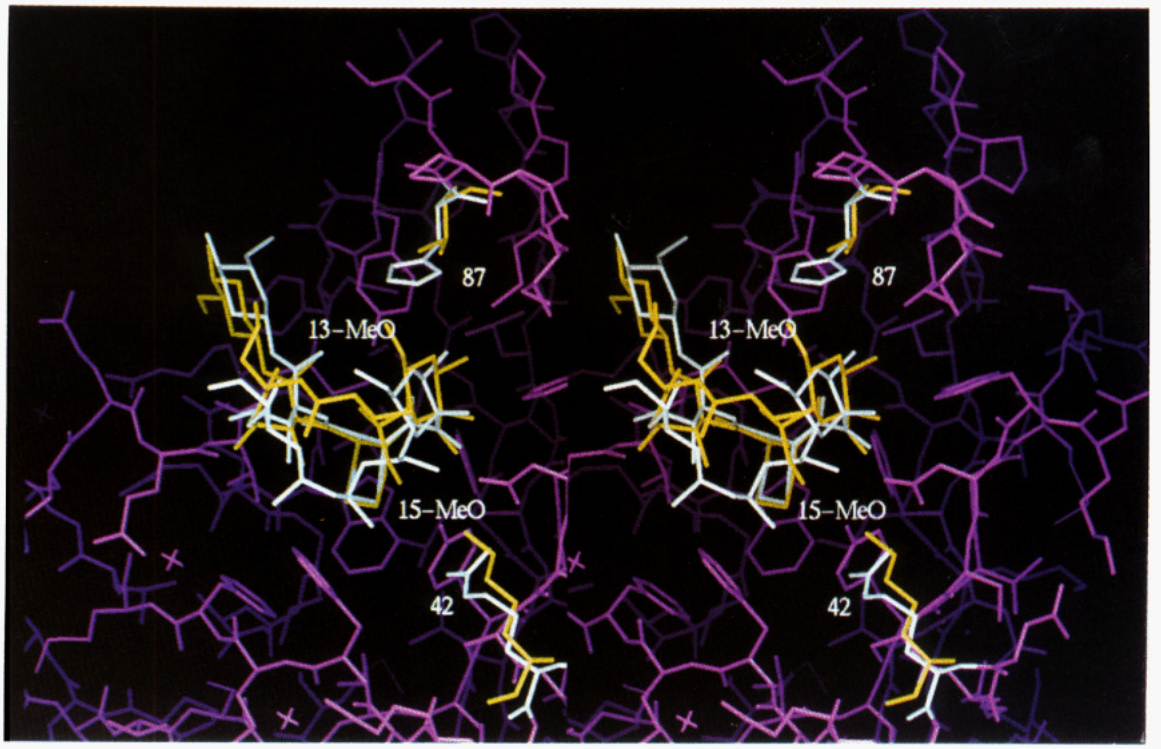

FIGURE 5: Model of the orientation of FK506 within the active site of R42K, H87V FKBP-12 (yellow), compared to the X-ray structure (white) of FK506 bound to wild-type FKBP-12 (Van Duyne et al., 1991, 1993). Superposition based on the protein backbone heavy atoms.

The differences between the NMR and X-ray structures may be attributed to perturbations of the solid-state structures by intermolecular crystal packing interactions. Less pronounced, but similar effects were observed previously upon comparing the NMR and X-ray structures of FK506 bound to the wild-type complex (Lepre et al., 1992). In the double mutant crystal, each FK506 molecule makes intermolecular contacts with two other ligand molecules, as well as with the side chains of residue 87 from two opposing protein molecules (S. Itoh, M. DeCenzo, R. Aldape, D. Livingston, D. Pearlman, and M. Navia, unpublished results). This illustrates an inherent problem with studying the X-ray structures of His 87 mutants in this crystal form: making one His 87 mutation in the protein is tantamount to making three substitutions, since each ligand contacts three side chains from residue 87 in the crystal. As a result, it may be impossible to separate the effects of mutation-induced changes in the crystal packing from those due to direct intramolecular effects. For this reason, the X-ray structures of FK506/FKBP-12 complexes obtained from this space group should be interpreted cautiously, unless other confirmatory data (*e.g.*, a structure determined in solution or from another space group) is available.

Direct comparison of the NMR solution structures of FK506 bound to double mutant and wild-type FKBP-12 reveals that the mutations induce local changes in the ligand conformation. Torsion angle changes in the macrocycle backbone from C14 to C19 move the backbone by 2.5 to 4.5 Å, and shift the orientations of 15-MeO and 17-Me by roughly 90° and 180°, respectively, relative to the wild-type orientation. The pyranose ring rotates slightly, shifting 13-MeO toward Val 87. The two families of TARMD structures are distinct, indicating that the ligand does not interconvert between the two conformations.

Analysis of the crystal structure of the wild-type complex reveals that the side chain of D37 forms a salt bridge with R42 and hydrogen bonds to the C10 hydroxyl of FK506 (Van Duyne et al., 1991, 1993). In the R42K and H87V single mutants, this salt bridge is absent and higher temperature factors are observed for the 36−46 loop, but the conformations of the protein and macrocycle are essentially the same as in the wild-type complex (S. Itoh, M. DeCenzo, R. Aldape, D. Livingston, D. Pearlman, and M. Navia, unpublished results). The results of the present work, however, show that the R42K, H87V double mutation induces changes in the FK506 backbone that are greater than those observed in the solid-state structures of either single mutant. Although the double mutations may decrease the inhibitory activity of the complex by perturbing residues that are directly recognized by calcineurin, the observed mutationally induced changes in the effector region alone could also be directly responsible for the reduction in calcineurin inhibition.

Because the mutationally induced structural changes of FK506 affect the entire region of the ligand that is bound between the Lys 42 and Val 87 side chains, the two mutations may act cooperatively to shift FK506 in the protein binding pocket. Figure 5 illustrates a possible structural mechanism for such a cooperative shift. This model is created by superimposing the NMR structure of FK506 bound to double mutant FKBP-12 upon the crystal structure of FK506 bound to wild-type FKBP-12, by using only the protein backbone heavy atoms. The pipecolinyl−dicarbonyl regions of the ligands are in good agreement, indicating that the superposition based upon the protein backbone works reasonably well for reproducing the relative ligand orientations. Since the NMR data only provide information about the ligand structure, the orientations of the Lys 42 and Val 87 side chains are presumed to be the same in solution as they are in the crystal structure (S. Itoh, M. DeCenzo, R. Aldape, D. Livingston, D. Pearlman, and M. Navia, unpublished results).

We propose the following explanation for the effect of the double mutation upon the ligand structure and, conse-

quently, upon the calcineurin affinity of the complex: In the wild-type complex, the side chain of Arg 42 bends to form a salt bridge with Asp 37. In the double mutant complex, this salt bridge is replaced by a hydrogen bond between Asp 37 and the terminal amine of Lys 42. This causes the Lys 42 side chain to extend farther than that of Arg 42, displacing 15-MeO and creating strain in the macrocycle backbone that induces changes in the C14 to C19 torsion angles. At the same time, the bulky aromatic ring of His 87 has been replaced by the smaller Val side chain, opening up a hydrophobic pocket that accepts the shifted methyl group of 13-MeO. It appears that both mutations are required to induce the full cooperative ligand shift: an extended side chain is necessary at residue 42 in order to create steric strain in the macrocycle, while a shorter side chain at residue 87 is needed in order to relieve this strain by permitting movement of 13-MeO. By altering the positions of essential groups in the ligand effector domain, these structural changes reduce the ability of the FK506/FKBP-12 complex to recognize and bind to calcineurin. Since many other pairs of mutations may be imagined that will combine a long side chain at residue 42 with a short side chain at residue 87, it should be possible to test the validity of this hypothesis with further mutagenesis experiments.

FK506 modulates both the structure and dynamics of FKBP-12 (Cheng et al., 1994), and is in turn influenced by the protein in the very regions that are believed to be important for calcineurin binding. From this study, it is apparent that the protein plays an active role in mediating the interaction between FK506 and calcineurin, not only by binding to FK506 in a manner that exposes the hydrophobic allyl region, but also by interacting directly with the macrocycle backbone in order to control the conformation of the effector region. This subtle interplay between FK506, FKBP-12, and calcineurin will continue to be of interest to those involved in the design of new immunosuppressive agents.

ACKNOWLEDGMENT

^{13}C-FK506 was produced by H. Kuboniwa and K. Munemura of Chugai Pharmaceuticals, Inc., using a germline kindly provided by K. Nagai at Tokyo Institute of Technology. Double mutant FKBP-12 was expressed by J. Fulghum and S. Chambers. We thank J. Griffith for providing software assistance and S. Itoh, J. Griffith, and M. Navia for access to crystallographic data prior to publication and for helpful discussions.

REFERENCES

Aldape, R. A., Futer, O., DeCenzo, M. T., Jarrett, B. P., Murcko, M. A., & Livingston, D. J. (1992) *J. Biol. Chem. 267*, 16029–16032.

Bierer, B. E., Somers, P. K., Wandless, T. J., Burakoff, S. J., & Schreiber, S. L. (1990) *Science 250*, 556–559.

Cheng, J.-W., Lepre, C. A., & Moore, J. M. (1994) *Biochemistry 33*, 4093–4100.

Clipstone, N. A., & Crabtree, G. R. (1992) *Nature 357*, 695–697.

Eccles, C., Billeter, M., Güntert, P., & Wüthrich, K. (1989) *Abstracts of the Xth Meeting of the International Society for Magnetic Resonance,* Morzine, France, July 16–21, p S50.

Fruman, D. A., Klee, C. B., Bierer, B. E., & Burakoff, S. J. (1992) *Proc. Natl. Acad. Sci. U.S.A. 89*, 3686–3690.

Galat, A., Lane, W. S., Standaert, R. F., & Schreiber, S. L. (1992) *Biochemistry 31*, 2427–2434.

Harding, M. W., Galat, A., Uehling, D. E., & Schreiber, S. L. (1989) *Nature 341*, 758–760.

Havel, T. F. (1991) *Prog. Biophys. Mol. Biol. 56*, 43–78.

Jin, Y. J., Albers, M. W., Lane, W. S., Bierer, B. E., Schreiber, S. L., & Burakoff, S. J. (1991) *Proc. Natl. Acad. Sci. U.S.A. 88*, 6677–6681.

Lepre, C. A., Thomson, J. A., & Moore, J. M. (1992) *FEBS Lett. 302*, 89–96.

Lepre, C. A., Cheng, J. -W., & Moore, J. M. (1993) *J. Am. Chem. Soc. 115*, 4929–4930.

Liu, J., Farmer, J. D. J., Lane, W. S., Friedman, J., Weissman, I., & Schreiber, S. L. (1991) *Cell 66*, 807–815.

Liu, J., Albers, M. W., Wandless, T. J., Luan S., Alberg, D. G., Belshaw, P. J., Cohen, P., MacKintosh, C., Klee, C. B., & Schreiber, S. L. (1992) *Biochemistry 31*, 3896–3901.

Meadows, R. P., Nettesheim, D. G., Xu, R. X., Olejniczak, E. T., Petros, A. M., Holzman, T. F., Severin, J., Gubbins, E., Smith, H., & Fesik, S. W. (1993) *Biochemistry 32*, 754–765.

Moore, J. M., Peattie, D. A., Fitzgibbon, M. J., & Thomson, J. A. (1991) *Nature 351*, 248–250.

Michnick, S. W., Rosen, M. K., Wandless, T. J., Karplus, M., & Schreiber, S. L. (1991) *Science 252*, 836–842.

O'Keefe, S. J., Tamura, J., Kincaid, R. L., Tocci, M. J., & O'Neill, E. A. (1992) *Nature 357*, 692–694.

Pearlman, D. A. (1994) *J. Biomol. NMR 4*, 1–16.

Pearlman, D. A., & Kollman, P. A. (1991) *J. Mol. Biol. 220*, 457–479.

Pearlman D. A., Case, D. A., Caldwell, J. C., Seibel, G. L., Singh, U. C., Weiner, P. & Kollman, P. A. (1991) *AMBER (UCSF), Version 4.0,* University of California, San Francisco.

Peattie, D. A., Harding, M. W., Fleming, M. A., DeCenzo, M. T., Lippke, J. A., Livingston, D. L., & Benasutti, M. (1992) *Proc. Natl. Acad. Sci. U.S.A. 89*, 10974.

Pranata, J., & Jorgensen, W. L. (1991) *J. Am. Chem. Soc. 113*, 9483–9493.

Rosen, M. K., & Schreiber, S. L. (1992) *Angew. Chem., Int. Ed. Engl. 31*, 384–400.

Rosen, M. K., Yang, D., Martin, P. K., & Schreiber, S. L. (1993) *J. Am. Chem. Soc. 115*, 821–822.

Rotonda, J., Burbaum, J. J., Chan, H. K., Marcy, A. I., & Becker, J. W. (1993) *J. Biol. Chem. 268*, 7607–7609.

Ryckaert, J. P., Ciccotti, G., & Berendsen, H. J. C. (1977) *J. Comput. Phys. 23*, 327–341.

Schreiber, S. L. (1991) *Science 251*, 283–287.

Siekierka, J. J., Hung, S. H., Poe, M., Lin C. S., & Sigal, N. H. (1989) *Nature 341*, 758–760.

Sigal, N. H., & Dumont, F. J. (1992) *Annu. Rev. Immunol. 10*, 519–560.

Torda, A. E., Scheek, R. M., & van Gunsteren, W. F. (1989) *Chem. Phys. Lett. 157*, 289–294.

Torda, A. E., Scheek, R. M., & van Gunsteren, W. F. (1990) *J. Mol. Biol. 214*, 223–235.

Van Duyne, G. D., Standaert, R. F., Karplus, P. A., Schreiber, S. L., & Clardy, J. (1991) *Science 252*, 839.

Van Duyne, G. D., Standaert, R. F., Karplus, P. A., Schreiber, S. L., & Clardy, J. (1993) *J. Mol. Biol. 229*, 105–124.

Yang, D., Rosen, M. K., & Schreiber, S. L. (1993) *J. Am. Chem. Soc. 115*, 819–820.